Linking Permafrost Deformation to Active Layer Freeze-thaw Dynamics in the Qinghai-Tibet Engineering Corridor

Supplementary materials:

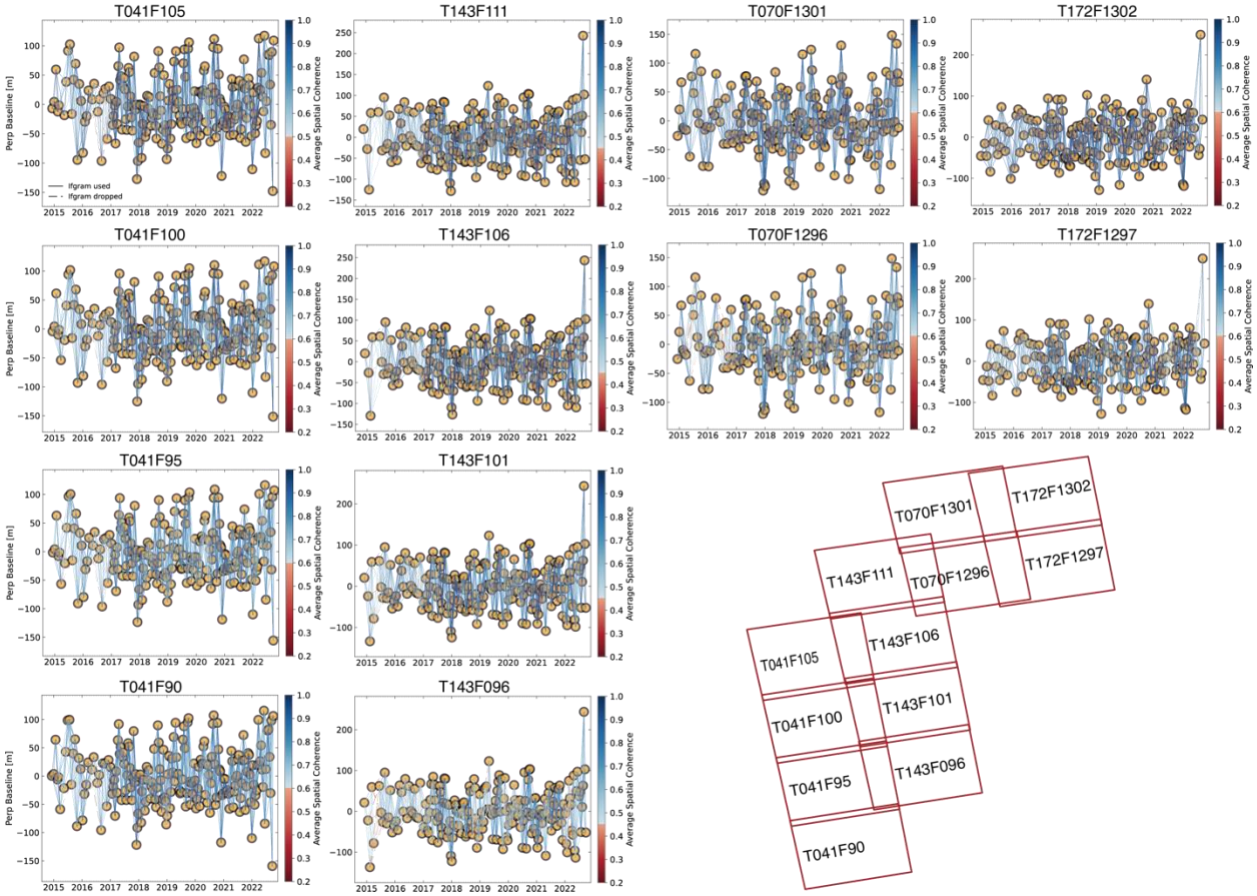

Figure S1. InSAR baseline network for the ascending Sentinel-1 tracks (T) and frames (F) encompassing the QTEC.

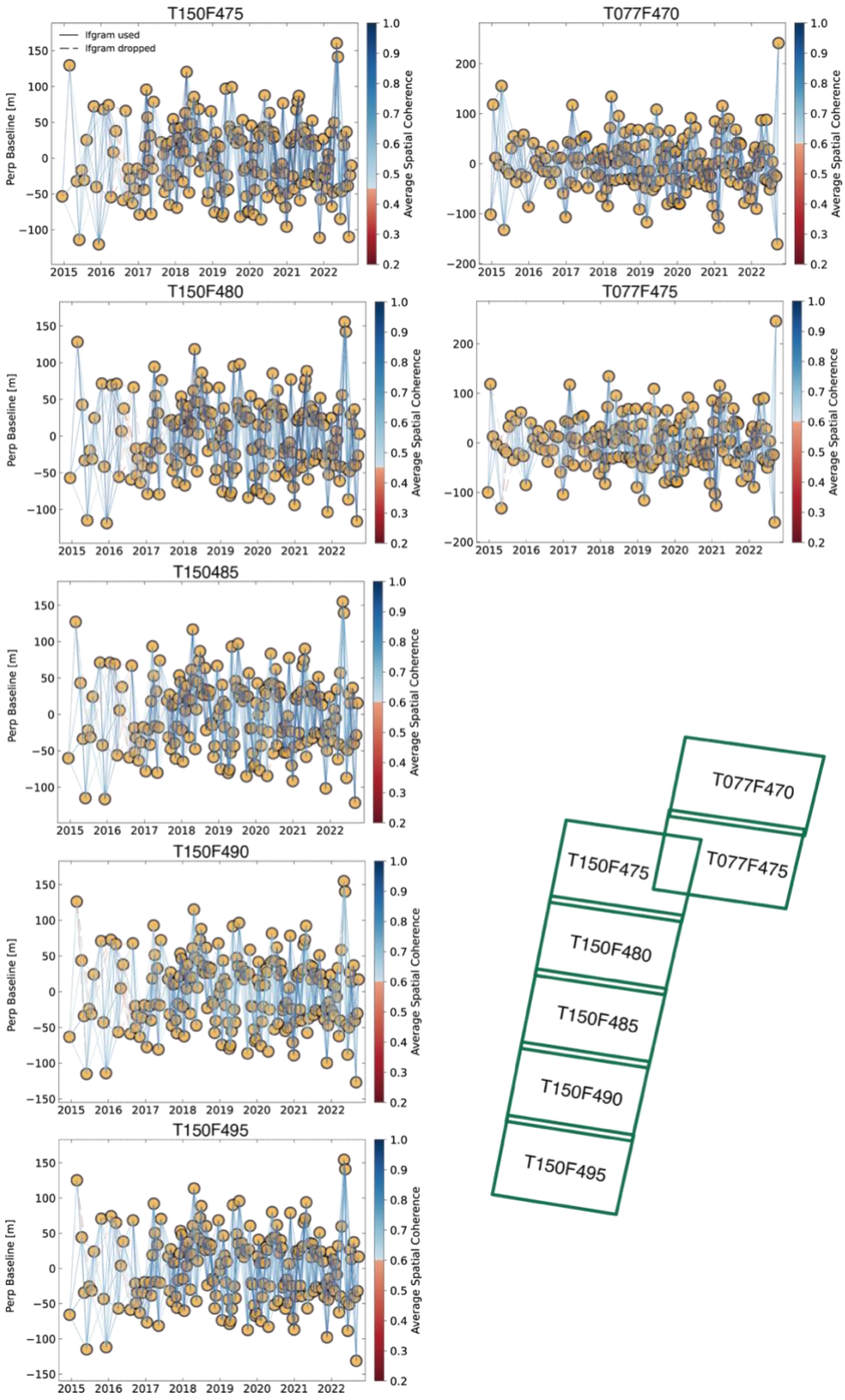

10 Figure S2. InSAR baseline network for the descending Sentinel-1 tracks (T) and frames (F) encompassing the QTEC.

Table S1. In-situ active layer thickness measurements used to constrain the volumetric water content in dry spring (n) in this study.

no.	lon	lat	station	ALT H_m	source of ALT H_m	sea_defo_m	N	n
1	94.09	35.72	XD13	2.8	Zhao & Sheng (2019)	0.0104	0.1247	0.0832
2	94.05	35.71	XD04	1.30		0.0061	0.1222	0.0704
3	94.12	35.71	XD11	2.30		0.0116	0.1229	0.0668
4	93.91	35.45	BQ03	3.30		0.0357	0.1356	0.0160
5	93.9	35.36	BQ04	3.40		0.0187	0.1402	0.0791
6	93.91	35.24	BQ06	2.90		0.0099	0.1372	0.0991
7	93.95	35.17	BQ02	2.80		0.0275	0.1380	0.0293
8	94.04	35.08	BQ07	1.90		0.0084	0.1429	0.0934
9	94.43	35.01	BQ11	2.10		0.0271	0.1589	0.0159
10	94.58	34.98	BQ13	3.20		0.0200	0.1799	0.1102
11	92.93	34.83	BLH	4.06	Chen (2018)	0.0177	0.2310	0.1821
12	92.92	34.86	BLR1	1.76	Qin et al. (2017)	0.0231	0.2206	0.0747
13	91.65	33.01	TGL	2.12		0.0105	0.1728	0.1174
14	92.9	34.77	FHS	1.70		0.0089	0.2524	0.1933
15	92.88	34.69	FH1	2.50	Wu et al. (2008)	0.0091	0.1850	0.1442
16	91.87	32.7	TG1	3.00		0.0343	0.2285	0.1009
17	94.05	35.62	KM2	1.83	Wu et al. (2012)	0.0144	0.1291	0.0417
18	93.96	35.62	BD1	2.47		0.0050	0.1292	0.1066
19	93.45	35.36	CM5	2.84		0.0364	0.1499	0.0082
20	93.22	35.28	CM7	4.80		0.0162	0.1564	0.1186
21	93.11	35.2	WD3	1.93		0.0233	0.1526	0.0190
22	93.03	35.07	HR3	2.36		0.0276	0.2046	0.0747
23	92.9	34.67	FH2	1.76		0.0119	0.1731	0.0978
24	92.74	34.58	YM1	3.32		0.0229	0.1582	0.0815
25	92.73	34.48	WL1	3.09		0.0224	0.1564	0.0758
26	92.34	34.01	KL1	2.40		0.0233	0.1655	0.0576
27	92.34	33.94	KL5	3.38		0.0147	0.1643	0.1156
28	91.75	33.07	TG4	2.77		0.0175	0.1770	0.1066
29	91.53	32.51	TJ1	3.50		0.0156	0.2278	0.1776
30	92.93	34.83	BL1	3.38	Wu et al. (2015)	0.0177	0.2310	0.1724
31	92.94	34.85	BL4	2.07		0.0214	0.2203	0.1050
32	92.94	34.84	BL6	2.48		0.0239	0.2244	0.1167
33	93.01	35.05	Yu-7	3.50	Wu et al. (2017)	0.0134	0.2213	0.1782
34	93.01	35.05	Yu-6	2.00		0.0134	0.2213	0.1461
35	92.9	34.73	CH1	1.65	Xie et al. (2012)	0.0239	0.2399	0.0787
36	92.73	34.47	CH3	2.80		0.0158	0.1560	0.0930
37	94.08	35.72	QTB1	1.65	Xie et al. (2015)	0.0104	0.1243	0.0541

38	93.27	35.29	QTB6	3.32		0.0057	0.1546	0.1353
39	91.9	33.1	QTB15	2.35		0.0191	0.1765	0.0859
40	93.58	35.41	DK1048+620	3.28	Niu (2021)	0.0307	0.1267	0.0230
41	93.09	35.22	QT08	2.42		0.0218	0.1567	0.0567
42	92.92	34.82	QT03	2.57	Zhao et al. (2021)	0.0345	0.2369	0.0872
43	92.89	34.73	Ch01	2.01		0.0107	0.2287	0.1692
44	92.34	33.96	QT05	3.19		0.0201	0.1579	0.0878

References for the Supplementary Materials:

Chen, J., Liu, L., Zhang, T., et al. (2018). Using persistent scatterer interferometry to map and quantify permafrost thaw subsidence: A case study of Eboling Mountain on the Qinghai-Tibet Plateau. *Journal of Geophysical Research: Earth Surface*, *123*(10), 2663–2676.

Niu, F. (2022). Demonstration monitoring data for disease treatment of permafrost project in South Asia Channel – long-term monitoring demonstration for subgrade stability of Chumar River of Qinghai Tibet Railway (2003–2021). National Tibetan Plateau Data Center National Tibetan Plateau Data Center. https://doi.org/10.11888/Cryos.tpdc.271933

Qin, Y., Wu, T., Zhao, L., et al. (2017). Numerical modeling of the active layer thickness and permafrost thermal state across Qinghai-Tibetan Plateau. *Journal of Geophysical Research: Atmospheres*, *122*(21), 11,604-11,620.

Wu, Q., Hou, Y., Yun, H. & Liu, Y. (2015). Changes in active-layer thickness and near-surface permafrost between 2002 and 2012 in alpine ecosystems, Qinghai–Xizang (Tibet) Plateau, China. *Glob. Planet. Change*, *124*, 149–155.

Wu, Q., Yu, W. & Jin, H. (2017). No protection of permafrost due to desertification on the Qinghai–Tibet Plateau. *Sci. Rep.*, *7*, 1544.

Wu, Q. & Zhang, T. (2008). Recent permafrost warming on the Qinghai-Tibetan Plateau. *Journal of Geophysical Research: Atmospheres*, *113*, D13108.

Wu, Q., Zhang, T. & Liu, Y (2012). Thermal state of the active layer and permafrost along the Qinghai-Xizang (Tibet) Railway from 2006 to 2010. *Cryosphere*, *6*, 607–612.

Xie, C., Zhao, L., Wu, T. & Dong, X. (2012). Changes in the thermal and hydraulic regime within the active layer in the Qinghai-Tibet Plateau. *J. Mt. Sci.*, *9*, 483–491.

Xie, C., William, A. G., Zhao, L., Wu, T. & Liu, W. (2015). Temperature-dependent adjustments of the permafrost thermal profiles on the Qinghai-Tibet Plateau, China. *Arct., Antarct., Alp. Res.*, *47*, 719–728.

Zhao, L. & Sheng, Y. (2019). Permafrost and Its Change on the Qinghai-Tibet Plateau. (Science Press).

Zhao, L., Zou, D., Hu, G., Wu, T., Du, E., Liu, G., Xiao, Y., Li, R., Pang, Q., Qiao, Y., Wu, X., Sun, Z., Xing, Z., Sheng, Y., Zhao, Y., Shi, J., Xie, C., Wang, L., Wang, C., & Cheng, G.

(2021). A synthesis dataset of permafrost thermal state for the Qinghai–Tibet (Xizang) Plateau, China. *Earth System Science Data*, *13*(8), 4207–4218.